AD NUMBER
AD013096
CLASSIFICATION CHANGES
TO: **unclassified**
FROM: **confidential**
LIMITATION CHANGES
TO: **Approved for public release; distribution is unlimited.**
FROM: **Distribution authorized to U.S. Gov't. agencies and their contractors; Administrative/Operational Use; MAY 1953. Other requests shall be referred to Office of Naval Research, Arlington, VA 22203.**
AUTHORITY
31 Dec 1965, DoDD 5200.10; ONR ltr, 29 Oct 1977

AD NUMBER
AD013096
CLASSIFICATION CHANGES
TO: **confidential**
FROM: **restricted**
AUTHORITY
ONR ltr, 10 Dec 1953

REPORT NUMBER
I-53-4

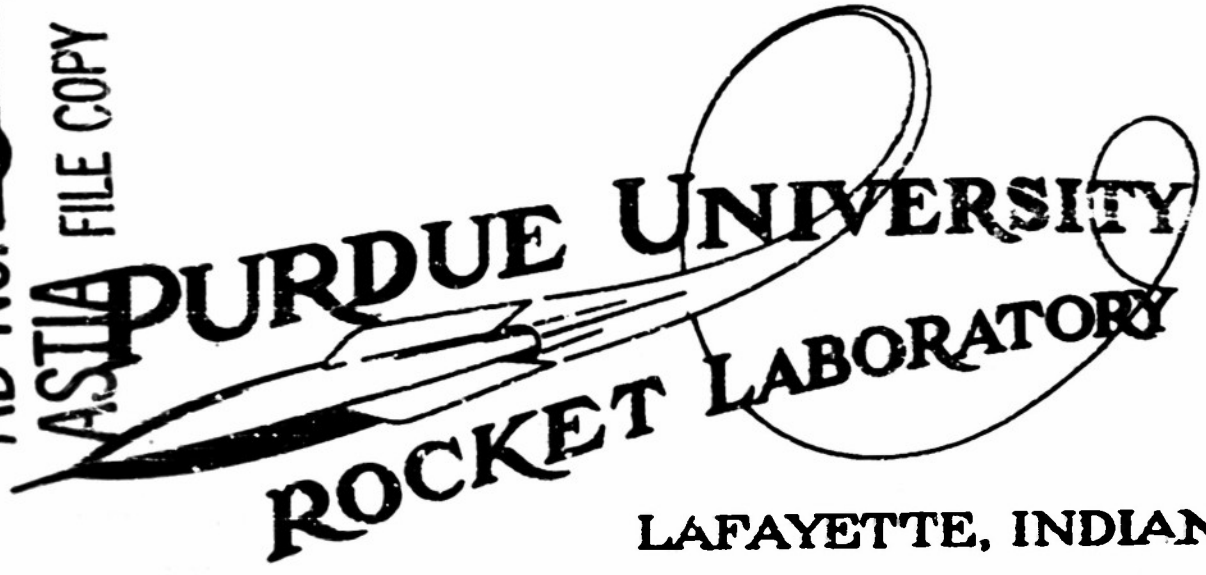

LAFAYETTE, INDIANA

EXPERIMENTAL ROCKET MOTOR PERFORMANCE WITH WHITE FUMING NITRIC ACID AND JP-4 AT 1000 PSIA COMBUSTION PRESSURE

Delbert E. Robison

Interim Report No. 3
Contract N7-onr-39418

ISSUE DATE
MAY 1953

PURDUE UNIVERSITY
AND
PURDUE RESEARCH FOUNDATION
Lafayette, Indiana

REPORT NO. I-53-4

EXPERIMENTAL ROCKET MOTOR PERFORMANCE WITH WHITE FUMING NITRIC ACID AND JP-4 AT 1000 PSIA COMBUSTION PRESSURE

Delbert E. Robison

Interim Report No. 3
Contract N7-onr-39416

ROCKET LABORATORY

May, 1953

TABLE OF CONTENTS

LIST OF FIGURES

ACKNOWLEDGEMENTS

The work reported herein was conducted under a research program sponsored by the Office of Naval Research Contract N7-onr-39415, Task Order 15.

The author is indebted to Dr. M.J. Zucrow for his counsel and assistance in preparing this report and his guidance in conducting the research work. He wishes also to express his appreciation to Dr. C.F. Warner and to Dr. C.M. Beighley for their technical advice and assistance. He is indebted to Mr. R.T. Tucker, Research Assistant, to Mr. R.E. Watters, Instrument Technician, and to the Test Mechanics of the Rocket Laboratory, Purdue University, for their assistance in conducting the experiments.

EXPERIMENTAL ROCKET MOTOR PERFORMANCE WITH WHITE FUMING NITRIC ACID AND JP-4 AT 1000 PSIA COMBUSTION PRESSURE

BY

Delbert E. Robison

I. INTRODUCTION

The research program, of which the experiments reported herein form a part, is concerned with obtaining experimental data pertinent to the performance and general characteristics of a rocket motor operating at high combustion pressures using white fuming nitric acid (WFNA) and jet propulsion fuel (JP-4) as the propellants. Some of the experiments were conducted using JP-3 as the fuel, and some using JP-4.

In addition to investigating rocket motor performance, average heat transfer rates were measured for the combustion chamber and the nozzle.

At least 95 per cent of the theoretical (frozen composition) values of specific impulse for the propellants was obtained at all mixture ratios by utilizing a triplet type injector in conjunction with a turbulence ring similar to the one described in reference 1.

II. PERFORMANCE AND HEAT TRANSFER AT 1000 PSIA COMBUSTION PRESSURE

Figure 1 presents the specific impulse I_{sp}, the thrust coefficient C_f, and the characteristic velocity C^*, uncorrected for the heat transferred to the cooling water, as functions of the mixture ratio[1]. The theoretical values for WFNA and n-octane, based on frozen equilibrium composition (references 4 and 5) are also presented for comparison. It is seen that the maximum values of specific impulse, thrust coefficient,

1. Mixture ratio = O/F = $\frac{\text{oxidizer weight flow rate}}{\text{fuel weight flow rate}}$

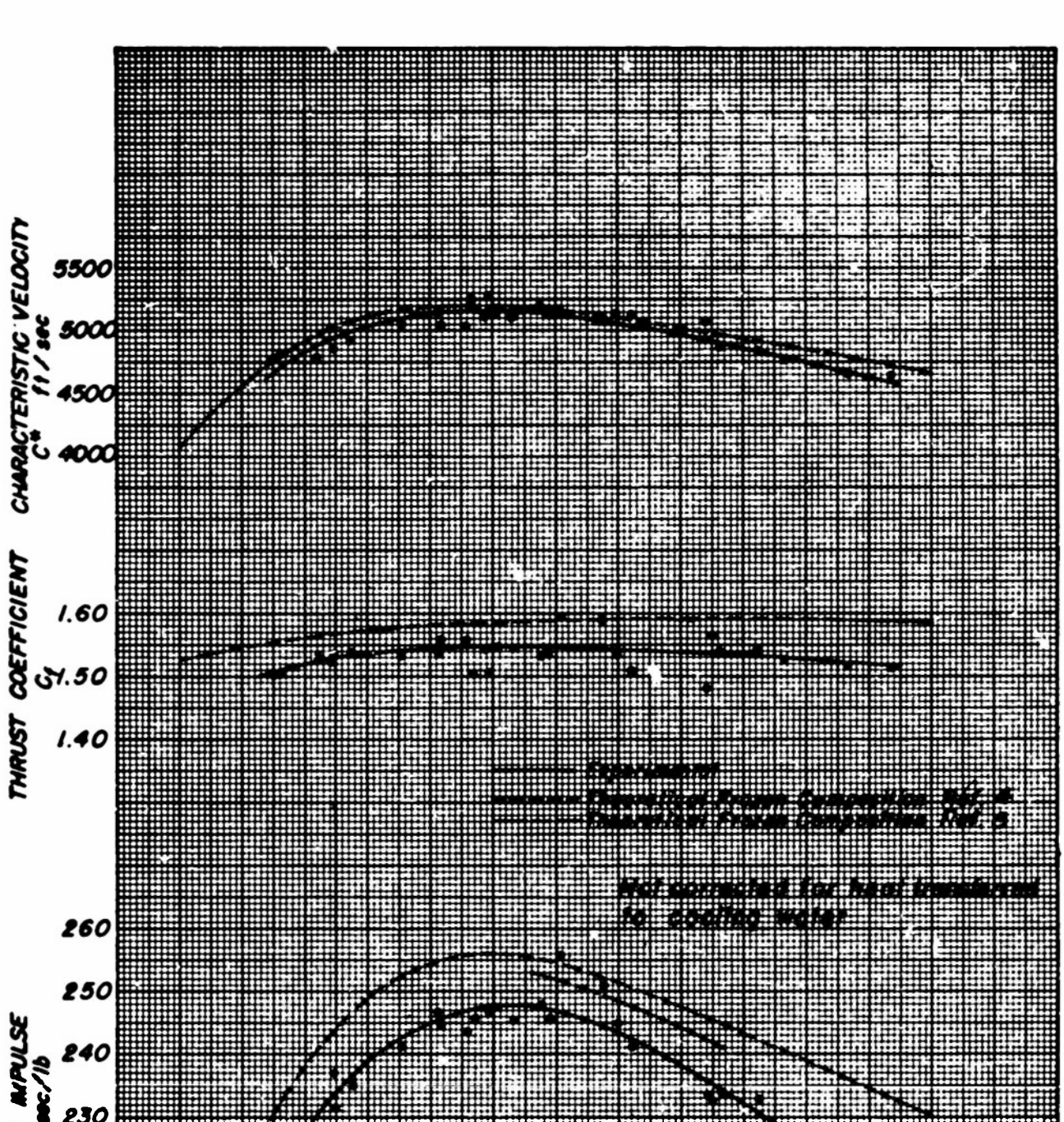

Fig. 1. Performance versus Mixture Ratio for WFNA and JP-4 at 1000 psia Combustion Pressure

and characteristic velocity occur at a mixture ratio of approximately 4.6. Their respective values are I_{sp} = 248 lb sec per lb, C_f = 1.55, and C^* = 5150 ft per sec.

Figure 2 presents the experimental specific impulse corrected for the heat transferred to the cooling water, I_{spc}, and is compared with the theoretical values mentioned above. A smooth curve drawn through the experimental points indicates that the maximum corrected specific impulse is 256 lb-sec per lb and occurs at a mixture ratio of 4.6. In the mixture ratio range 4 to 5.5 there is little difference between the experimental values of I_{sp} and the theoretical values.

In the mixture ratio ranges 2.8 to 4 and 5.5 to 7.8 the experimental values of I_{sp} are smaller than the theoretical values, and the difference between the two values tends to increase as the mixture ratio departs from the optimum value of 4.6. Since one injector, in conjunction with a turbulence ring, was employed over the entire mixture ratio range of 2.8 to 7.8, the differential pressures acting on the oxidizer and fuel orifices differed widely at the extreme limits of the mixture ratio range. For example, the pressure drop across the fuel orifices decreased from 200 psi for a mixture ratio of 3 to 50 psi for a mixture ratio of 7, while the corresponding pressure drops for the oxidizer orifices increased from 120 psi to 245 psi. It seems reasonable to assume from previous work conducted at this laboratory that if the experiments had been conducted with several injectors, each designed for the particular mixture ratio being studied, the difference between the corrected experimental values of I_{sp} and the theoretical values would be much smaller.

When the rocket motor was operated with rich mixture ratios below 3, the combustion tended to be rough, but no serious instability was encountered. "Smooth" sounding, stable operation was obtained in the mixture ratio range of 3 to 5. With mixture ratios leaner than 5.5, unstable combustion was generally encountered, but not always. Stable operation was obtained at leaner mixture ratios with the first 6-point

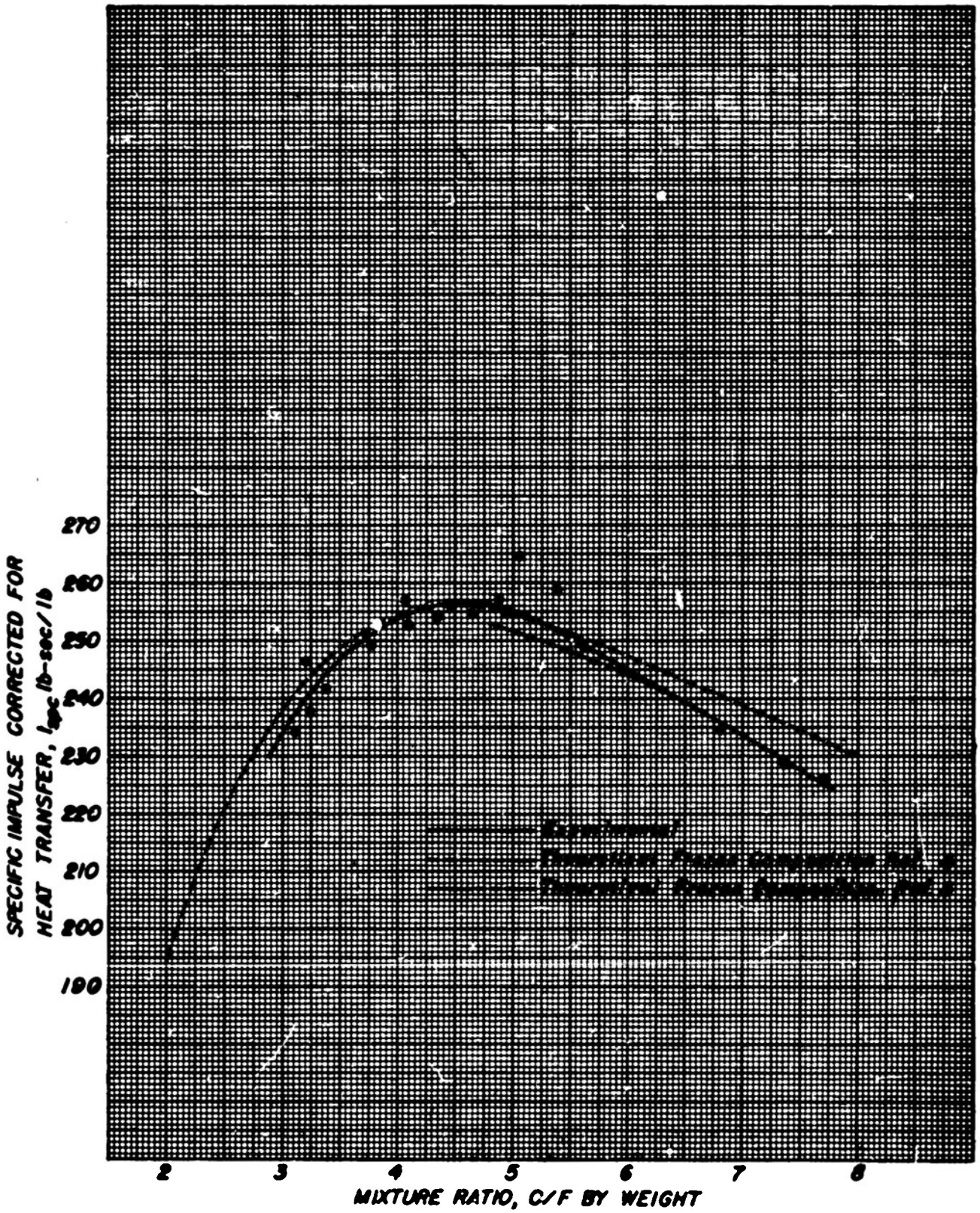

Fig. 2 Specific Impulse Corrected for Heat Transfer vs Mixture Ratio for WFNA and JP-4 at 1000 psia Combustion Pressure.

injector (2:1-6T-1) employed than with the second (2:1-6T-2). The only difference between the two injectors was that the pressure drops across the second was slightly lower.

Figure 3 presents the average heat transfer fluxes for the combustion chamber, the nozzle, and the over-all heat transfer flux for the rocket motor. The over-all heat transfer flux is defined as the ratio of the sum of the nozzle and the combustion chamber heat transfer rates to the combined inside surface area of the two components. The over-all heat transfer flux does not include the heat transferred (approximately 6 per cent of the total) to the turbulence ring.

Although the data presented in Fig. 3 are somewhat scattered, the dependency of heat transfer on mixture ratio is quite evident. The trend of the data indicates that the maximum value for the average heat transfer flux for the nozzle was 8.3 B/sec-in^2 and occurred at a mixture ratio of 4.8. The average heat transfer flux for the combustion chamber was a maximum at a mixture ratio of 4.5, having the value 4.2 B/sec-in^2.

The detailed experimental data obtained at 1000-psia combustion pressure are tabulated in Table 1, Appendix A.

III. EFFECT OF COMBUSTION PRESSURE ON PERFORMANCE AND HEAT TRANSFER

It is of interest to compare the performance of rocket motors operating at 1000-psia combustion pressure with that of motors operating at combustion pressures of 300, 500, and 700 psia. The performance of WFNA and JP-3 for the latter combustion pressures is presented in references 1 and 2, and was obtained under the same program as the 1000-psia data reported herein. Geometrically similar motors, each developing 500 pounds thrust, were employed throughout the program.

The effect of combustion pressure on the corrected specific impulse for mixture ratios of 3.0, 4.5, and 6.0 is shown in Fig. 4. Except for p_c = 1000 psia and O/F=4.5, the experimental values are all lower than the theoretical values, the average differences being 1.4 per cent for a mixture ratio of 4.5, and 3.6 per cent for mixture ratios of 3.0 and 6.0. The experimental specific impulse may not represent the maximum values that can be attained for mixture ratios of 3 and 6. They do, however, represent the performance that can be expected if one injector is employed for

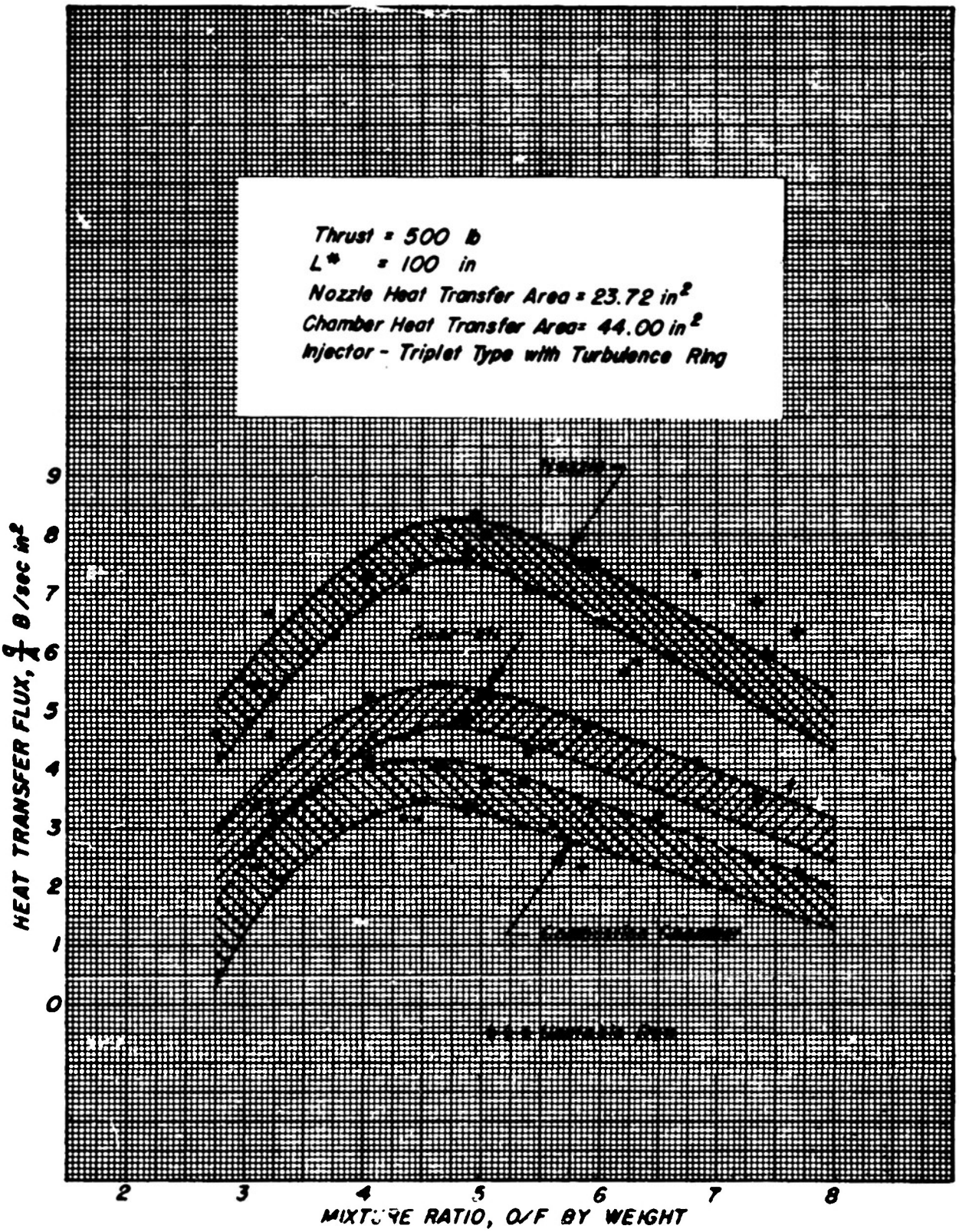

Fig. 3 Heat Transfer Flux vs Mixture Ratio For WFNA and JP-4 at 1000 psia Combustion Pressure

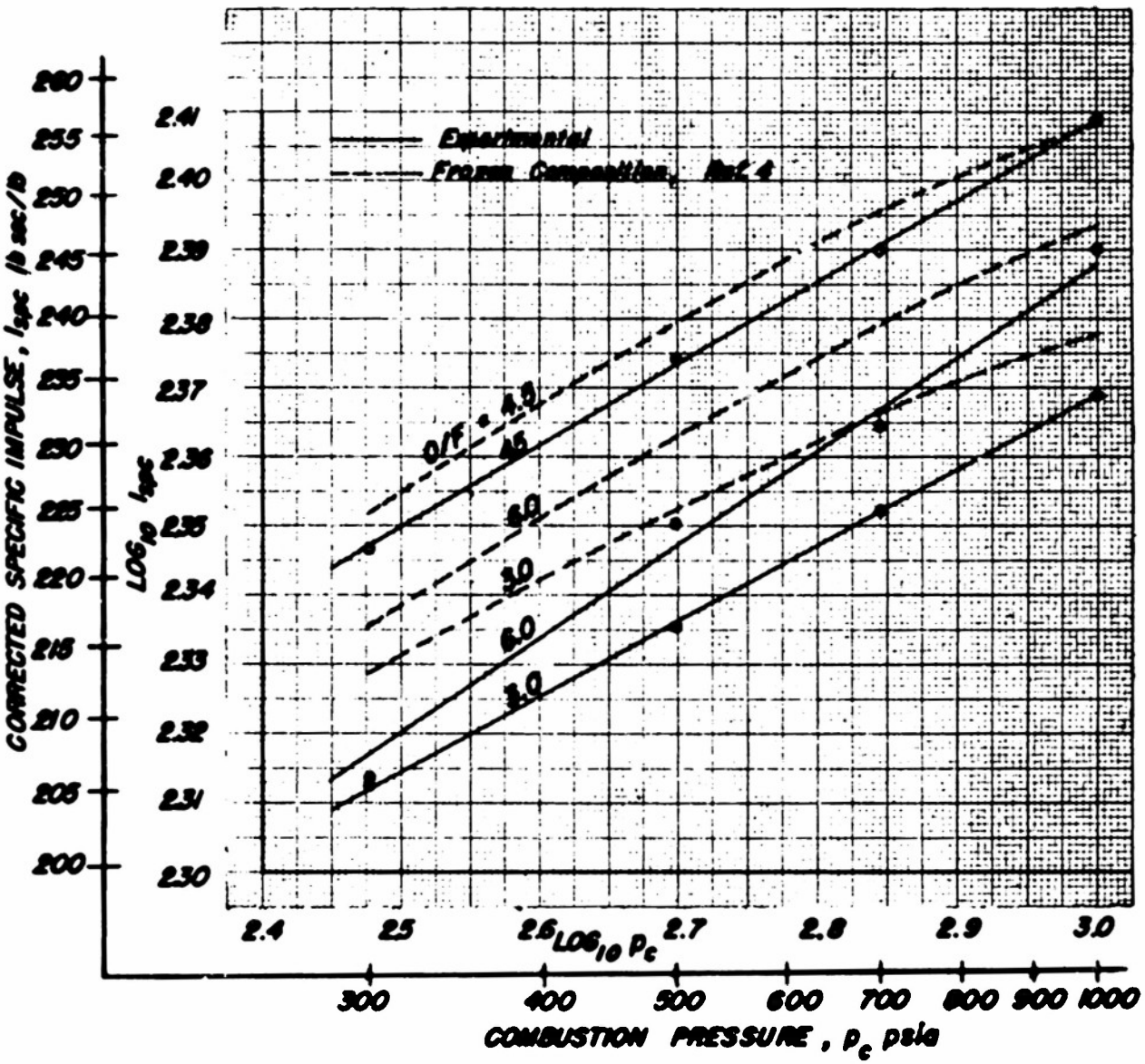

Fig. 4. Variation of Specific Impulse Corrected for Heat Transfer with Combustion Pressure at Different Mixture Ratios.

the mixture ratio range of 3 to 6.

The variation of the experimentally determined specific impulse with combustion pressure is represented closely by the exponential curve

$$(I_{spc})_1 = (I_{spc})_2 \left(\frac{p_{c1}}{p_{c2}}\right)^n = C p_c^n \qquad (1)$$

in which C is a constant and n is the slope of the experimental curve. Both the exponent n and the constant C have different values for different mixture ratios.

Employing two points on each experimental curve shown in Fig. 4, the following equations were determined for the combustion pressure range of 300 to 1000 psia. For the optimum mixture ratio 4.5, the maximum corrected specific impulse is given by

$$I_{spc} = 113.2\ p_c^{0.1184} \pm 0.5 \text{ lb-sec/lb} \qquad (2)$$

For the mixture ratio 3.0,

$$I_{spc} = 110.2\ p_c^{0.1090} \pm 0.5 \text{ lb-sec/lb} \qquad (3)$$

and for the mixture ratio 6.0

$$I_{spc} = 95.91\ p_c^{0.1353} \pm 1.7 \text{ lb-sec/lb} \qquad (4)$$

Figure 5 shows the effect of combustion pressure on the heat transfer. The shaded areas represent the maxima and minima, due to scattering of the data for the peak heat transfer flux, for combustion pressures of 300, 500, 700, and 1000 psia. At each pressure, the maximum average heat transfer flux was obtained in the mixture ratio regime 4.5 to 5. The maximum heat transfer fluxes for the nozzle and the combustion chamber at 1000 psia are both approximately 3 times the respective values measured at 300 psia.

The experimentally determined heat transfer fluxes are represented within $\pm$ 0.5 B.sec-in^2 by the following linear equations:

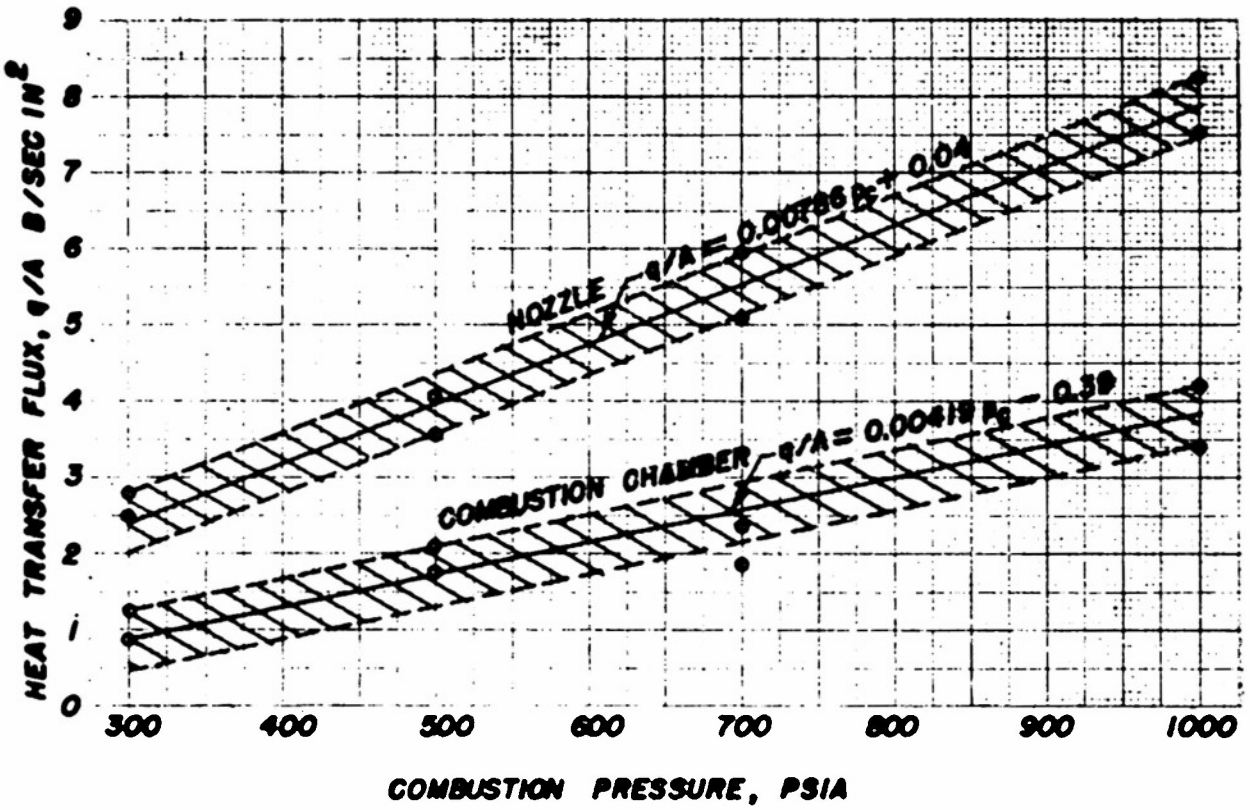

Fig. 5. Variation of Maximum Heat Transfer Flux with Combustion Pressure.

$$\text{Nozzle, } q_n/A_n = 0.00786p_c + 0.04 \tag{5}$$

$$\text{Chamber, } q_c/A_c = 0.00419\ p_c - 0.39 \tag{6}$$

It is interesting to note that the nozzle heat transfer flux is essentially directly proportional to the combustion pressure, and that within the scatter of the experimental data, the combustion chamber heat transfer flux could also be considered as being proportional to the combustion pressure.

During the course of the experimental work a short investigation was made of the suitability of available ceramic materials as liners for the combustion chamber and nozzle of a 500 lb thrust rocket motor operating at 1000-psia. All of the ceramic liners failed in less than one second of operation, but the ceramic lined combustion chambers were undamaged after firing durations of 10 seconds. No effort was made, however, to establish the life of those liners.

IV. CONCLUSIONS

1. The maximum performance of a rocket motor operating on WFNA and JP-4 at 1000-psia combustion pressure and producing 500 pounds thrust occurs in the mixture ratio regime 4 to 5. More specifically, the trends of the experimental curves indicate that a maximum specific impulse of 256 lb-sec/lb can be obtained at a mixture ratio of 4.6. This is a 4.5 per cent increase above the maximum value obtained at 700-psia combustion pressure, and 15.4 per cent greater than the maximum value obtained at 300-psia combustion pressure.

2. The theoretical specific impulse based upon the frozen equilibrium compositions given in reference 4 closely approximates the experimental corrected values in the mixture ratio regime 4 to 5.5. For mixture ratios less than 4 and greater than 5.5, the experimental values were lower; e.g., 3 per cent less at a mixture ratio of 7.5, and 1.7 per cent less at a mixture ratio of 3.0. The departure of the experimental performance from the theoretical values for mixture ratios above and below the optimum range may have been due to poor mixing provided by the injector.

It may, therefore, be possible to improve the performance at the extreme mixture ratios by employing an injector designed for the required mixture ratio.

3. For the combustion pressure range 300 to 1000 psia, with mixture ratios between 3 and 6, the specific impulse corrected for the heat transferred to the cooling water can be represented within 1 per cent by the exponential equation

$$I_{spc} = C\, p_c^{\,n}$$

in which C and n are constants which depend on the mixture ratio.

4. The maximum average heat transfer fluxes obtained at 1000-psia combustion pressure for the nozzle and the combustion chamber are both approximately 3 times those obtained at 300 psia. Within the experimental error, the nozzle and combustion chamber heat transfer fluxes can be expressed as linear functions of combustion pressure, and are both almost directly proportional to the combustion pressure.

5. No difference between the performance of JP-4 and WFNA and that of JP-3 and WFNA was detected.

6. It appears that as good performance can be obtained with a 6-impingement point triplet injector as with a 12-impingement point triplet injector when either is employed in conjunction with a turbulence ring.

7. It is difficult to obtain stable combustion throughout the complete mixture ratio range of 2.8 to 7.8 with only one injector. Unstable combustion occurred more frequently for mixture ratios leaner than 5.5. To operate over such a wide range of mixture ratios with one injector and still maintain supercritical pressure drops across the injector orifices may require differential pressure of the order of 300 to 400 psi at the extreme ends of the range. It is realized that the phenomenon of instability is not as yet well understood, and that the injector pressure drop and the quality of the mixing of the propellants after injection may

or may not be the principal cause of the combustion instability.

8. A water-cooled copper nozzle can be employed satisfactorily at 1000-psia combustion pressure with a coolant flow rate of approximately 1 lb per sec, and a pressure drop of approximately 760 psi. It appears, however, that the copper nozzle will require some type of external support, for example from the filler block, to prevent buckling.

9. None of the ceramic materials tested is satisfactory for the nozzles of uncooled rocket motors which are to operate at maximum performance at 1000-psia combustion pressure.

10. It may be possible that ceramic liners may withstand the conditions prevalent in the combustion chamber, but more experimental information is required to establish that conclusion.

V. DESCRIPTION OF EXPERIMENTAL ROCKET MOTORS

Four rocket motors, each having an L^* of 100 and designed to produce 500 pounds thrust, were employed for the investigation conducted at 1000-psia combustion pressure. Three of the motors were uncooled and were utilized for obtaining starting-up characteristics and preliminary performance information. One of the uncooled motors consisted of a niafrax combustion chamber and nozzle cemented in a mild steel retainer. The second uncooled motor comprised a "Borolite I" nozzle and combustion chamber cemented in a mild steel retainer. The third uncooled motor consisted of a stainless steel combustion chamber and a solid copper nozzle.

The fourth motor was water cooled and was the one employed for obtaining all of the performance and heat transfer data reported herein. Figure 6 is a cross-section through the experimental motor. Figure 7 is a photograph giving an exploded view of the motor assembly. The combustion chamber comprised an AISI type 347 stainless steel cylinder with helical grooves machined in the outer surface to form a helical coolant passage of rectangular cross section. Two combustion chambers of the latter design were employed during the investigation.

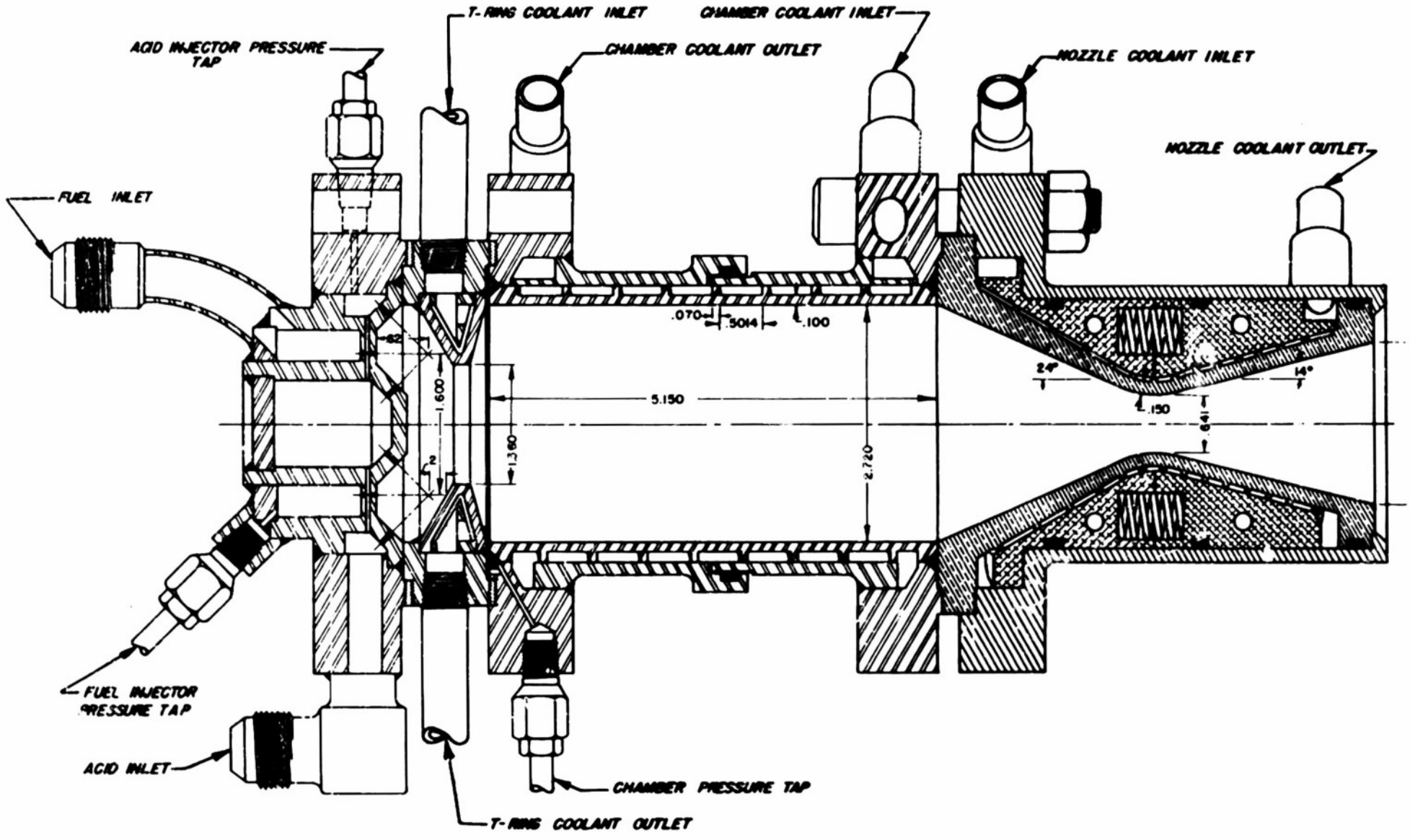

FIG. 6. Cross Section of 1000-psia Water-Cooled Rocket Motor

Three water-cooled copper nozzles were employed in the course of the investigation. One nozzle employed a helical coolant passage formed by silver soldering copper wire to the outer wall of the copper liner. That design proved to be unsatisfactory because the high coolant pressure deformed the wire thereby obstructing the coolant passage. In the two other copper nozzles the helical coolant passages were machined in their outer walls. Figure 8 illustrates the method employed for introducing the cooling water around the nozzle. The arrangement shown provides a uniform decrease in cross-sectional area of the coolant passage from the coolant inlet section to the wall of the copper nozzle, and in addition eliminates stagnation of the coolant at the inlet and outlet sections.

Three triplet-type injectors were employed during the course of the experiments; one had 12 impingement points, and two had 6 impingement points. The general configuration is illustrated in Fig. 6. Acid is ejected from the outer and inner circles of holes, while fuel is ejected from the circle of holes located between the two. All of the reported data were obtained with a triplet-type injector operating in conjunction with a turbulence ring. Each injector was designed to provide a pressure drop greater than 50 psi for the mixture ratio regime 3 to 7. The pressure drop versus flow rate characteristics for the turbulence ring and for each injector are presented in Figs. 9, 10, 11 and 12. The type of impingement and the resulting spray pattern produced with water by the 12-point injector is shown in Fig. 13. The photograph was taken before the injector was employed for a firing test. Figure 14 is a photograph of the spray pattern produced by the same injector when equipped with a turbulence ring.

VI. DESCRIPTION OF APPARATUS AND INSTRUMENTATION

Except for the following changes, the test apparatus employed for the experiments reported herein was identical to that described in references 1 and 2.

A Waterman flow control valve was installed at the coolant outlet section of the combustion chamber, and was adjusted to provide a flow

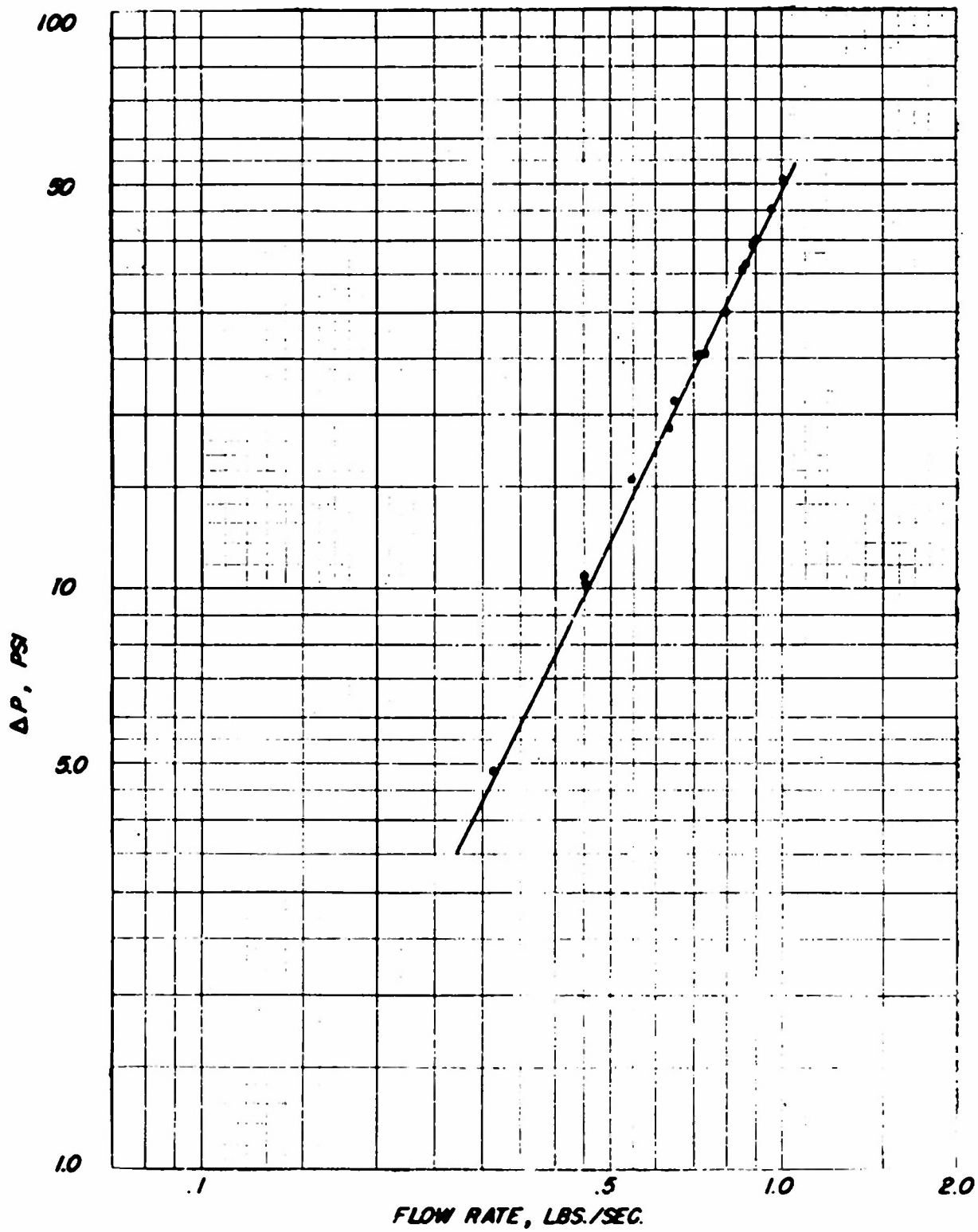

Fig. 9. Pressure Drop vs. Flow Rate for 1000 psi Turbulence Ring.

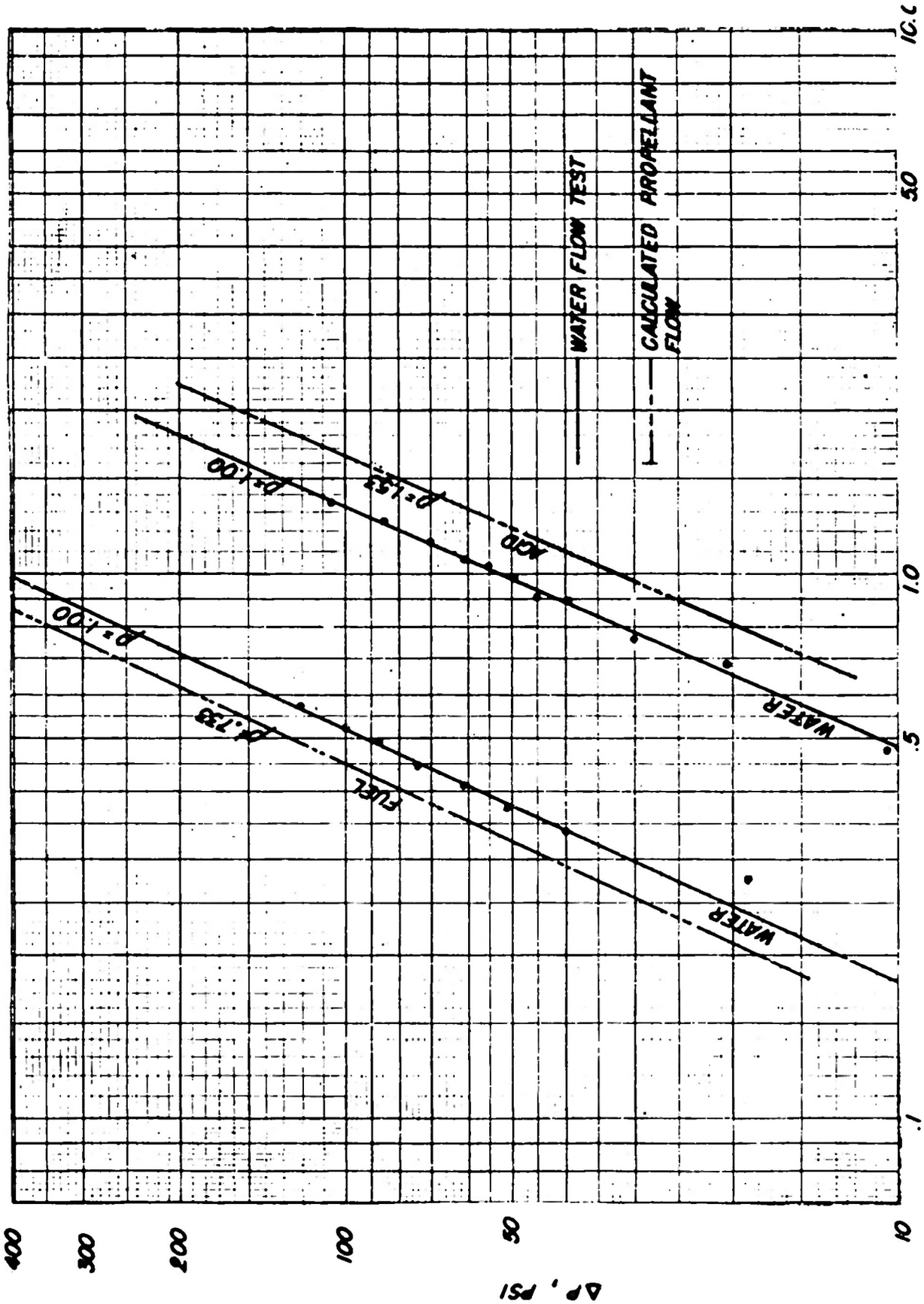

Fig. 10. Pressure Drop vs. Flow Rate for Injector 1000-2:1-12.

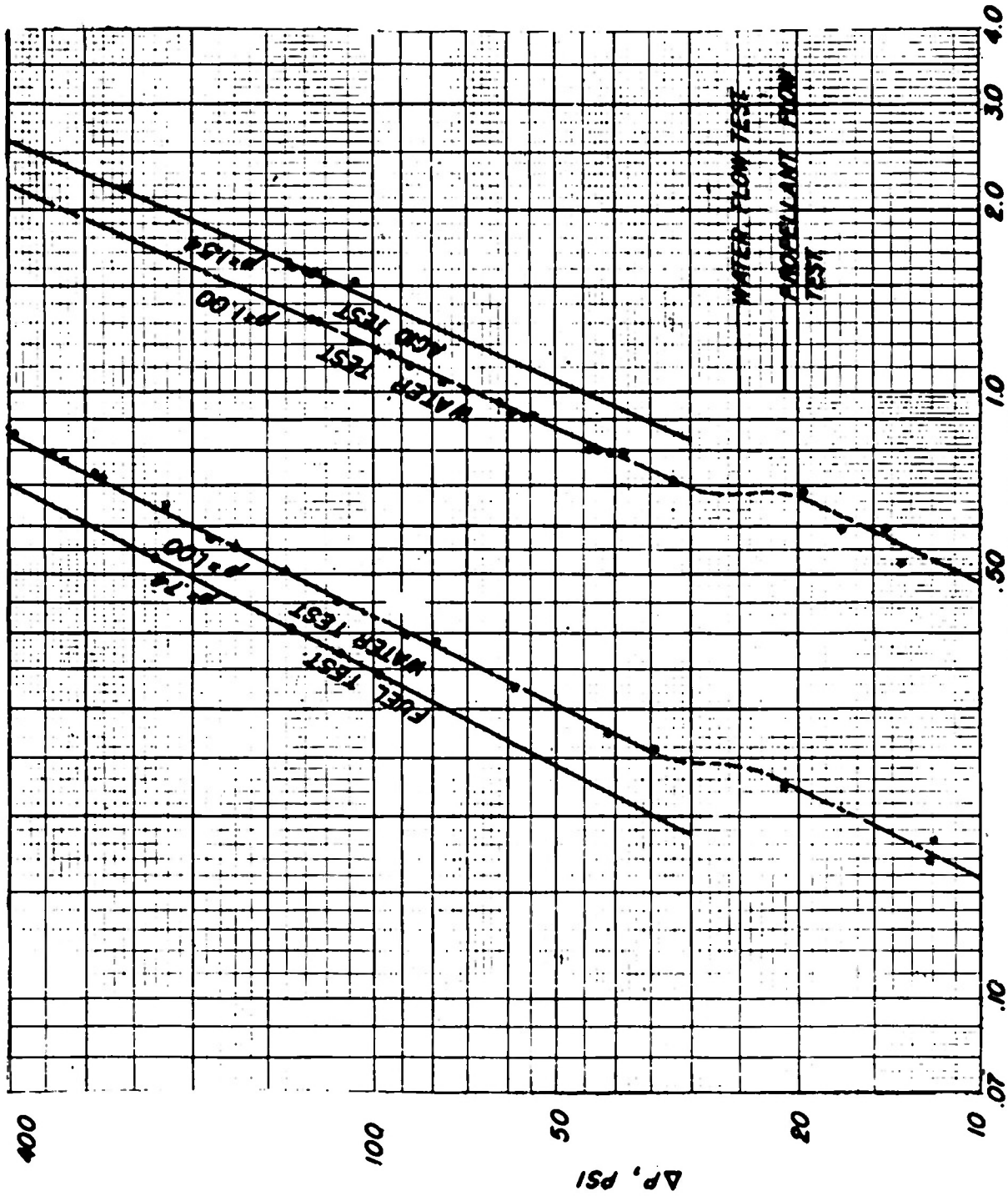

Fig. 11. Pressure Drop vs Flow Rate for Propellant Injector 1000-2:1-6-1.

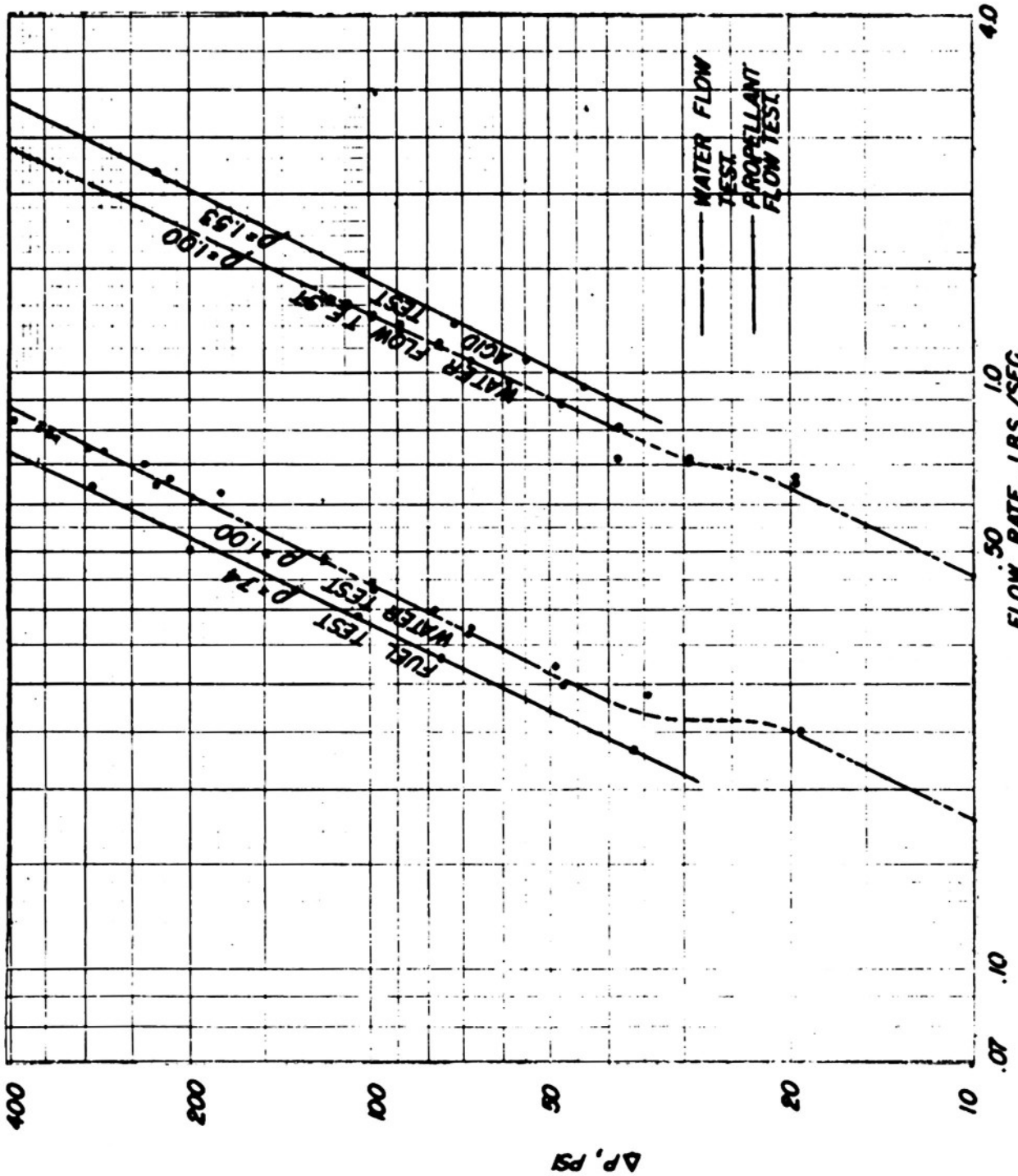

Fig. 12. Pressure Drop vs. Flow Rate for Propellant Injector 1000-2:1-6-2.

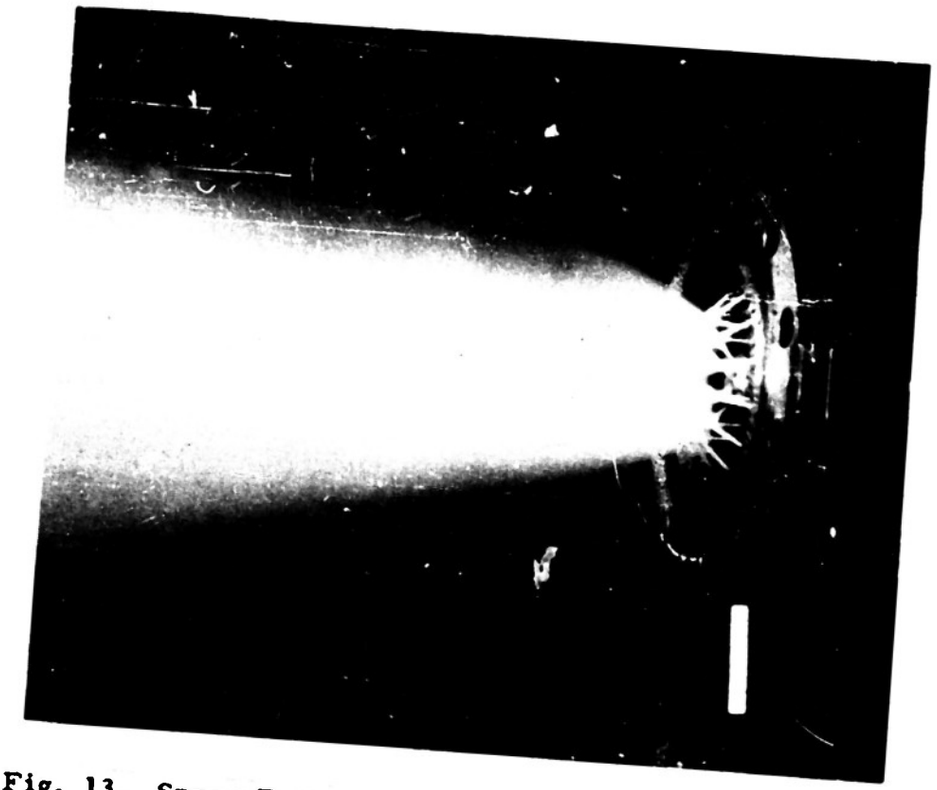

Fig. 13. Spray Pattern Produced by 1000-2:1-12 Injector

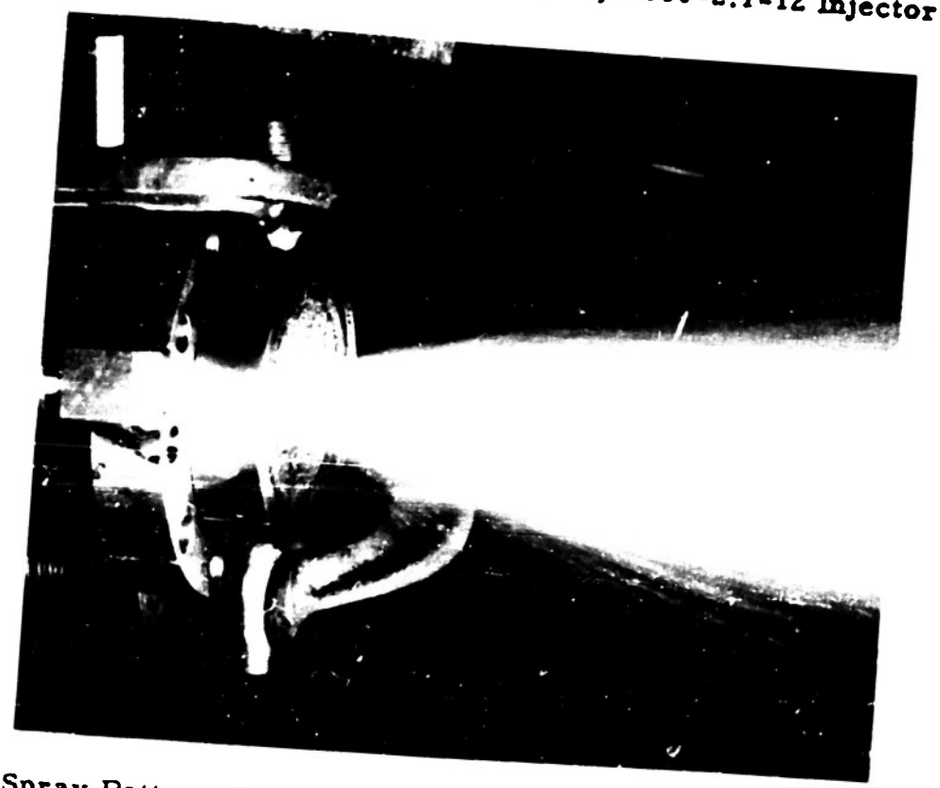

Fig. 14. Spray Pattern Produced by 1000-2:1-12 Injector and Turbulence Ring.

rate of 1 lb per sec, an inlet pressure of approximately 400 psia, and an outlet pressure of 230 psig. The coolant (water) for the combustion chamber was supplied by a centrifugal pump.

An air-pressurized cooling system was utilized for supplying cooling water to the nozzle. The flow rate was adjusted to approximately 1 lb per sec by means of a hand valve connected to the nozzle coolant outlet. The coolant pressure was adjusted to approximately 1000 psig at the inlet and 200 psig at the outlet. Since the coolant supply tank was pressurized from the same compressed air supply used for pressurizing the oxidizer supply tank, the nozzle coolant pressure and flow rate varied slightly from one firing test to the next depending upon the propellent mixture ratio.

The bipropellant valve employed was salvaged from XKL13-AJ-5 JATO unit and was modified to provide a more positive shut off and a slower opening speed. The pintles were redesigned in the manner previously described in reference 3.

Reluctance type transducers, described in references 1 and 3 were employed for measuring pressures, differential pressures, and thrust. The flows of coolant water to the nozzle and combustion chamber were measured by means of Flowrators, and the flow of coolant water to the turbulence ring calculated by means of Fig. 9 from measurements of the upstream coolant pressure during the run. All other flows were measured with sharp-edge orifices in conjunction with reluctance type differential pressure transducers. A more detailed discussion of the instrumentation and testing procedures employed is presented in reference 3.

VII. DISCUSSION OF EXPERIMENTS

Runs 172 to 180 were made primarily to obtain information concerning the operating characteristics of the entire system. The first run (Run 172) at 1000-psia combustion pressure was made with an uncooled motor (steel combustion chamber and copper nozzle) to obtain starting-up characteristics. The motor started smoothly, but a minor explosion occured

on shut-down. For run 173, the water cooled combustion chamber was employed. The combustion chamber performed satisfactorily, but the uncooled copper nozzle burned out in less than 5 seconds. A water-cooled nozzle was installed and the motor was run at 700-psia combustion pressure. The nozzle burned out at the throat after 35 seconds of operation. Judging from the position of the scale deposit in the coolant passage, the "burnout" was caused by boiling of the coolant. Runs 175 to 179 were made with the ceramic motors to obtain more complete information on operating characteristics. All of the ceramic nozzles burned out at the throat in less than 10 seconds. In most instances the burnout started in less than one second. Figure 15 is a photograph of one of those nozzles after firing showing the burnout as viewed from the divergent end of the nozzle.

A water-cooled copper nozzle (WC-Cu-1) was installed for Run 180. After 3 sec of running the nozzle coolant flow rate decreased and the motor was shut down. Choking of the coolant flow due to the generation of steam in the coolant passage appeared to be the cause of the decrease in the coolant flow rate.

A larger coolant flow rate was employed for Run 181. The motor performed satisfactorily for 24 sec. After the shut down, however, a small hole was discovered in the nozzle just downstream from the throat. Disassembly of the nozzle showed that the high coolant pressure had forced the copper nozzle away from the filler block, and had allowed the coolant to by-pass the coolant passage. Evidence of boiling was present in the region of the burnout. The coolant passage of the latter nozzle was formed by silver soldering a copper wire around the copper nozzle.

For Runs 182 to 187 a copper nozzle (WC-Cu-2) having machined coolant passages and a uniform wall thickness (0.15 in) was employed. That nozzle performed satisfactorily for run durations up to 39 sec. After Run 187 the nozzle had become deformed due to the high coolant pressure to which it had been exposed. It was replaced by a new nozzle (WC-Cu-3) which was designed with a tapered wall to improve its ability to resist collapse when exposed to high coolant pressures. The deformation occurred

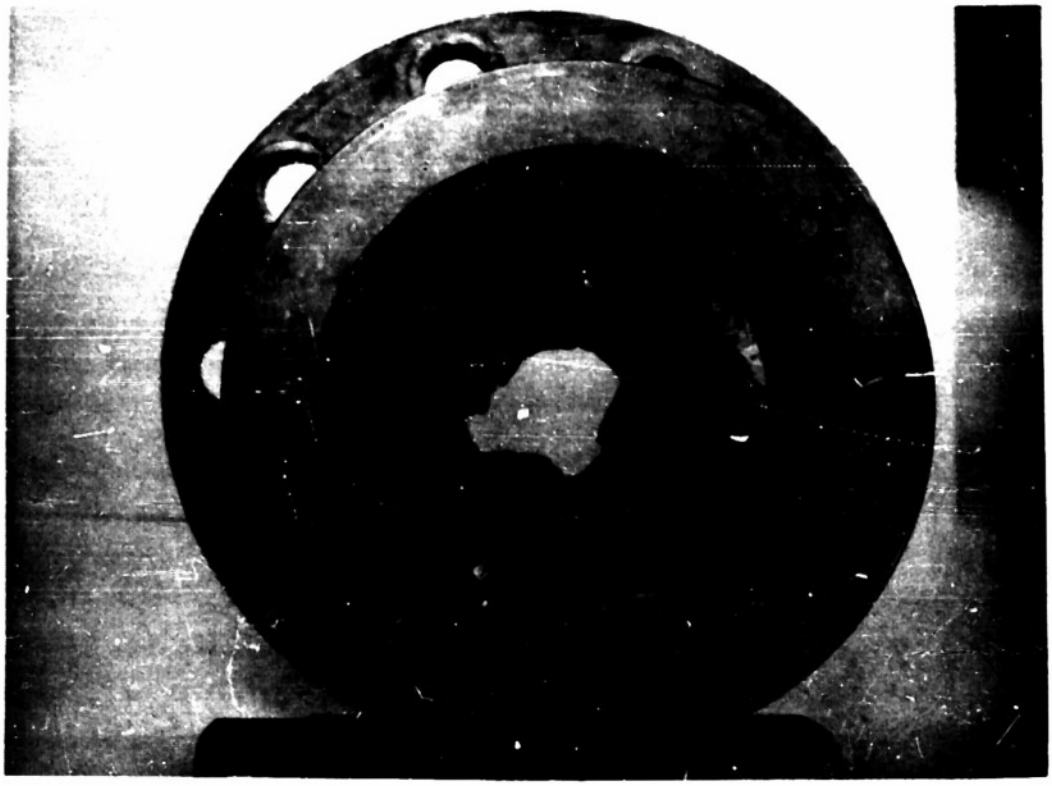

Fig. 15. Divergent Section of Ceramic Nozzle Showing Burnout at Throat

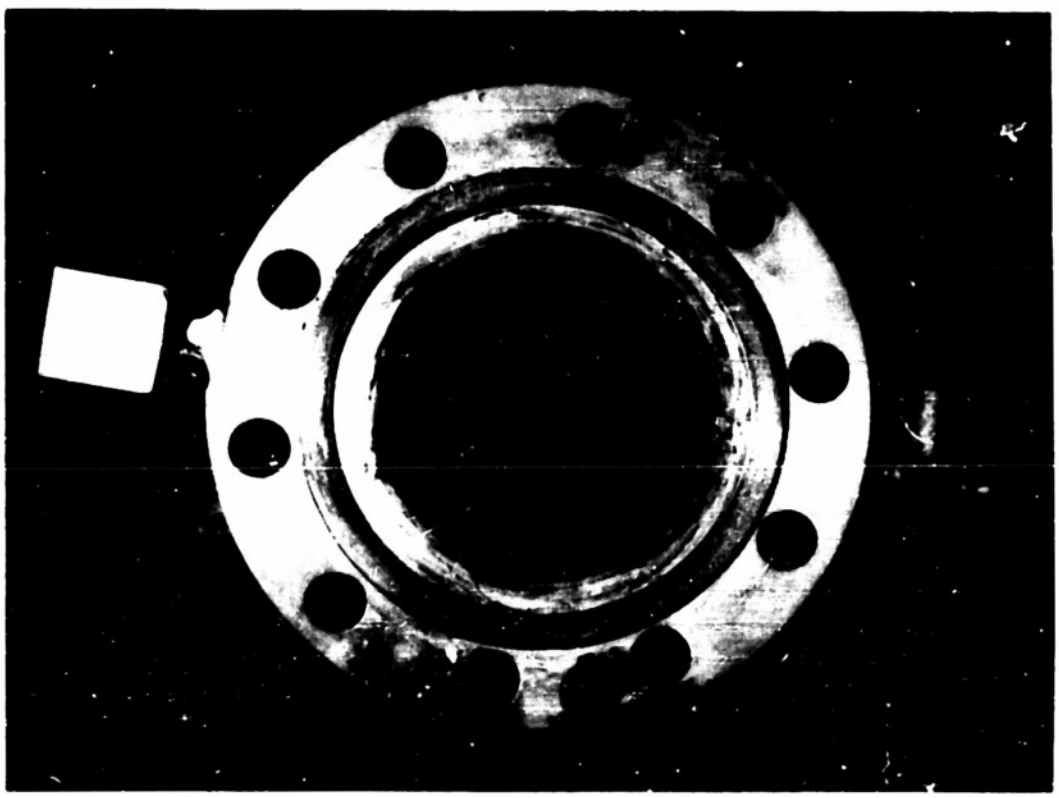

Fig. 16. 6-point Injector Showing Burned Area Around Injection Orifices

principally at shut-down when the nozzle was hot, and was unsupported by the gas pressure.

The thickness of the wall was increased to 7/16 in at the combustion chamber end, tapered uniformly to 0.212 in at the throat, and then increased uniformly to 0.25 in at nozzle exit. A 1/16 in deep coolant passage was machined in the outer wall of the nozzle. The nozzle assembly included a split filler block, equipped with springs, for holding the block firmly against the lands of the coolant passage. Figure 6 illustrates the nozzle assembly. Satisfactory operation of the nozzle design presented in Fig. 6 was obtained throughout the remainder of the investigation (Runs 188 to 204). The above mentioned design did not totally prevent the copper nozzle from creeping away from the filler block. After approximately three or four runs it was generally necessary to force the copper lands back against the filler block. This was done by driving two iron cones simultaneously into the converging and diverging sections of the nozzle.

A 12-impingement point triplet-type injector was employed for Runs 172 to 187. Slight burning of the injector face in the region of the fuel holes occured during each run. Moreover, the small fuel holes employed with the aforementioned injector tended to plug up with carbon; the small holes were required to produce a reasonable pressure drop across the fuel holes. Whether the plugging occurred during the starting-up period, during the run, or at shut-down was not determined.

To overcome the plugging of the fuel holes encountered with the 12-point injector, the latter was replaced by a 6-point triplet injector (2:1 -6T-1). The latter was designed to provide a higher pressure drop across the injection orifices and better cooling of the downstream face of the injector. Injector 2:1-6T-1 was employed for Runs 189 to 195. Figure 16 shows the injector face after it had been used for 7 runs. A small amount of burning occurred principally around the inboard acid orifices. The burning appeared to stop after it had progressed to a depth of approximately 0.05 in, leaving a wall thickness of approximately 0.1 inch.

An explosion caused by leakage of the starting fuel (furfuryl-alcohol mixed with aniline) into the acid manifold occurred on Run 195, and the injector manifold section was damaged beyond repair. The manifold section was replaced with another of identical design. Measurements of the pressure drops across the acid and fuel holes of the new injector showed them to be somewhat smaller than those for the previous injector for the same flow rates (see Figs. 11 and 12). A bipropellant valve salvaged from a YRL13-A J-5 JATO unit was modified to prevent leakage of the propellants into the injector manifolds by including O-ring seals in the pintles. In addition, the Teflon seats were replaced with aluminum seats. The redesigned bipropellant valve operated satisfactorily for the remainder of the investigation, Runs 196 to 204.

JP-3 was used as the fuel for Runs 172 to 193. For Runs 194 to 204 inclusive the fuel was JP-4. No distinguishable differences were observed in the starting-up, the combustion, and the performance characteristics of JP-3 and JP-4.

VIII. EXPERIMENTAL ERROR

The calculations of performance and heat transfer for the rocket motors were made on an IBM card program computing machine in the manner previously described in reference 3.

The method employed for estimating the accuracy of the experimental performance is also discussed in detail in reference 3. Employing the customary differential calculus method for small errors, the expected maximum error in the performance parameters were calculated for Run 204 by means of the IBM computer, the errors being 1.5 per cent for the specific impulse, 1.4 per cent for the thrust coefficient, and 1.9 per cent for the characteristic velocity. Though the errors vary slightly from one run to the next, they are of the same order as these given above.

For the data employed in Figures 1 and 2, the maximum deviation of the combustion pressure from 1000 psia was 2.9 per cent; however, the average deviation was 1.0 per cent. The maximum scatter of specific

impulse due to the deviation of combustion pressure is from equation 2 (see also Fig. 4) $\pm$ 0.9 sec and the average scatter is 0.3 sec for a mixture ratio of 4.6. Thus the effect of the deviation in combustion pressure from 1000 psia is within the accuracy of the experimental measurements.

Figures 1 and 2 do not include the runs which are marked with an asterisk in Table 1, Appendix A. Some of the runs so marked were utilized only for testing the starting-up characteristics of the motor. In others, instrumentation or mechanical failure in the system produced unreliable information. It may be noted in the comments of Table 1 that instability was encountered during the runs which are marked with a double asterisk. In many instances during an unstable period of the run the variation of propellant flow rate and coolant temperature was so large and so rapid that the respective recording instruments could not respond accurately. Figure 17 shows the oscillograph record of Run 202, and illustrates the transition from unstable to normal combustion. During the run the combustion alternated to and from unstable operation several times with no definite period of transition. For comparison a smooth run is shown in Fig. 18.

The inability of the recording potentiometer to record the pressure drop across the metering orifice employed for determining the propellant flow rate when unstable combustion was encountered, is illustrated in Fig. 19. Figure 19 shows the trace of the oxidizer metering orifice pressure drop obtained from a stable run (Run 204), and the trace from an unstable run (Run 202). The stable and unstable periods can be detected easily by comparing the trace with the oscillograph record in Fig. 17. During stable operation (normal combustion oscillation) the trace is relatively flat, but during unstable operation the trace wanders or drifts. Judging from the oscillograph record, particularly that of the nozzle coolant temperature (potentiometer trace not shown), the trace produced by the recording potentiometer because of its drifting character does not indicate the correct average value of the flow rate, but rather indicates the inability of the recorder to assume an average value when there are combustion vibrations.

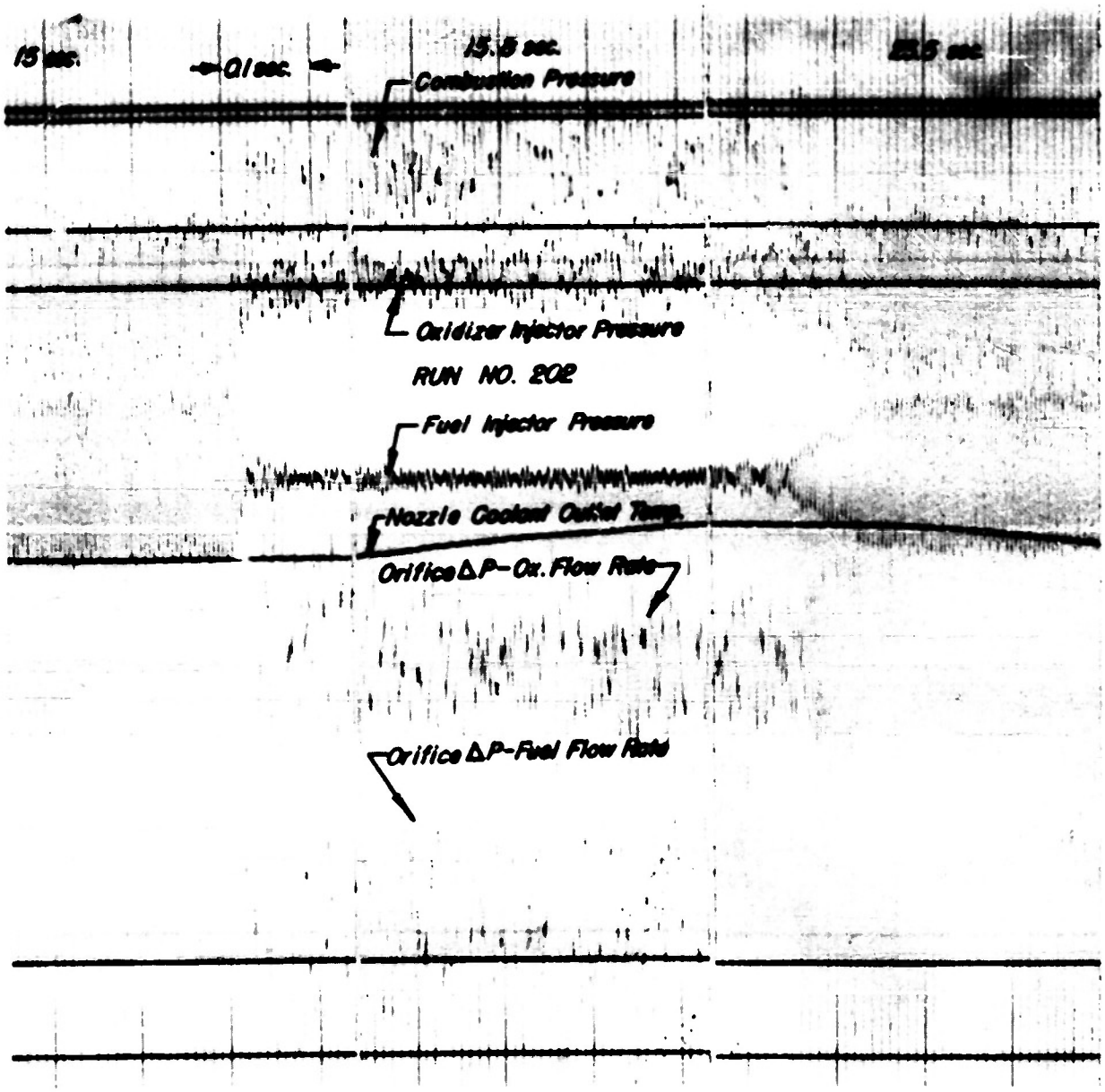

Fig. 17. Oscillograph Record of Unstable Run.

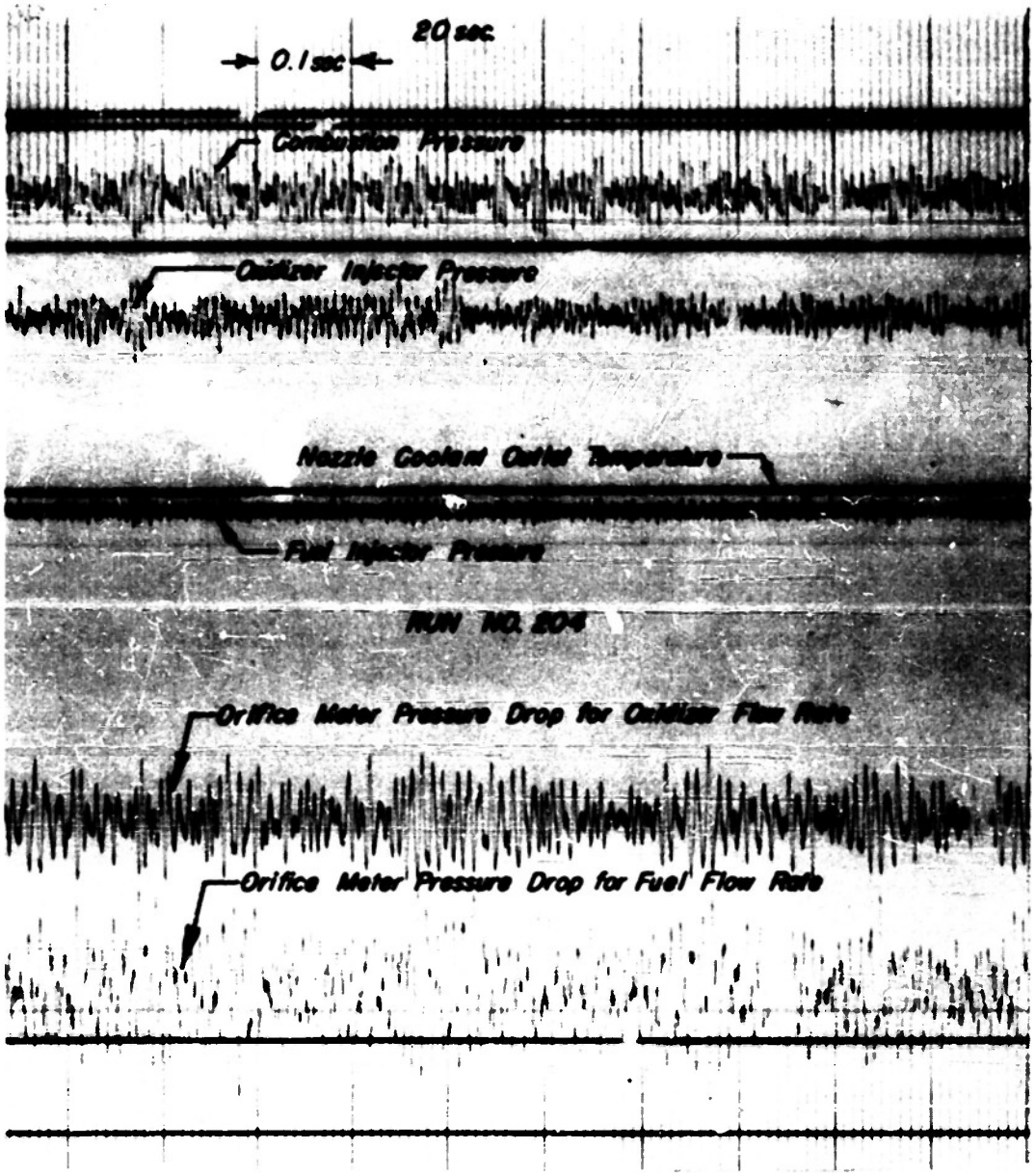

Fig. 18. Oscillograph Record of Stable Run

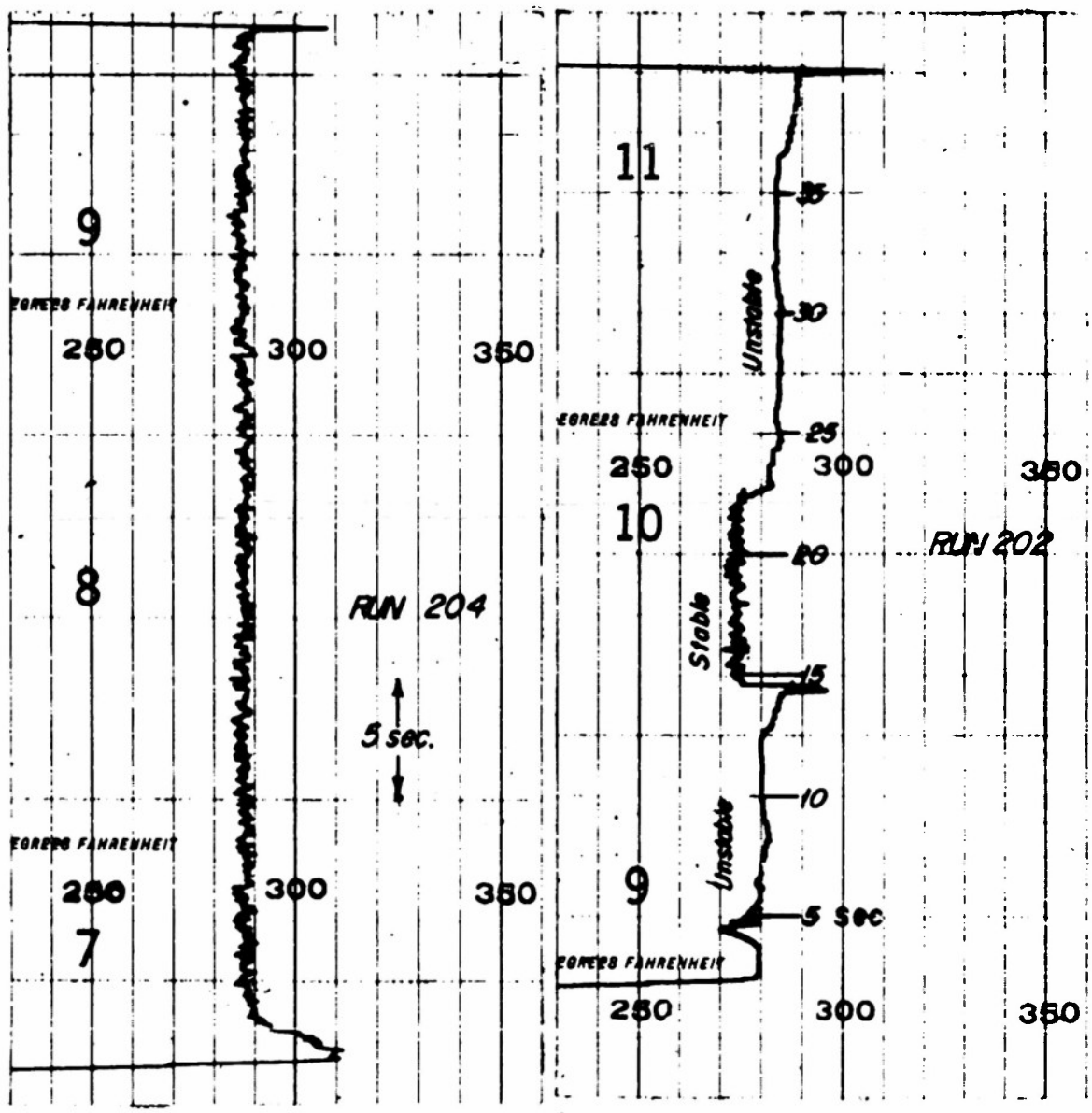

Fig. 19. Recording Potentiometer Trace of Pressure Drop for Acid Flow Rate Orifice Meter Illustrating a Stable and Unstable Run.

LIST OF SYMBOLS

A_c = surface area of combustion chamber

A_n = surface area of nozzle

C = constant

C_f = thrust coefficient

C^* = characteristic velocity

F = thrust

G_a = oxidizer flow rate

G_f = fuel flow rate

G_p = total propellant flow rate

I_{sp} = specific impulse

I_{spc} = specific impulse corrected for heat transfer

n = constant

O/F = ratio of oxidizer flow rate to fuel flow rate

p_c = combustion pressure

q_c = combustion chamber heat transfer rate

q_n = nozzle heat transfer rate

q_{tr} = turbulence ring heat transfer rate

REFERENCES

1. Beighley, C.M., "Experimental Rocket Motor Performance with White Fuming Nitric Acid and JP-3 at 500-psia Combustion Pressure," Purdue University and Purdue Research Foundation, Lafayette, Indiana, Rocket Laboratory Rept. No. 1-52-1, April 1952.

2. Beighley, C.M. and Robison, D.E., "Experimental Rocket Motor Performance with White Fuming Nitric Acid and JP-3 at 700 and 300 psia Combustion Pressure," Purdue University and Purdue Research Foundation, Rocket Laboratory Rept. No. 1-52-2, May 1952.

3. Beighley, C.M. and Robison, D.E., "Testing and Design Procedures High Combustion Pressure Rocket Motors," Purdue University and Purdue Research Foundation, Rocket Laboratory Rept. No. RM-53-2, April 1953.

4. Brinkley, Stuart R., "Equilibrium Composition, Thermodynamic Properties and Rocket Motor Performance of Octane-White Fuming Nitric Acid Systems," Explosives and Physical Sciences Division, U.S. Bureau of Mines, Rept. No. 3261, February 1953.

5. Trent, C.H., and Zucrow, M.J., "The Calculated Performance of Hydrocarbon White Fuming Nitric Acid Propellants at High Chamber Pressure," Project Squid, Tech. Memo. No. PUR-6, Purdue University, Lafayette, Indiana, March 1949.

APPENDIX A

Table 1. Performance and Heat Transfer Data for 1000 psia Combustion Pressure

Run No.	Date	Chamber No.	Nozzle No.	Injector No.	Run Time sec	Data Time Aver. sec	Chamber Pressure P_c psia	Thrust F lb	Axial Flow Rate $\dot{w}_f$ lb/sec	Fuel Flow Rate $\dot{w}_f$ lb/sec	Total Propellant Flow Rate $\dot{w}_p$ lb/sec	Mixture Ratio R	Specific Impulse I_{sp} lb-sec/lb	Nozzle Throat Area A_t in^2	Characteristic Velocity c^* ft/sec	Thrust Coeff. C_f	Heat Transfer Rate $\sqrt{A_c}$	$\frac{A_c+A_t}{A_t+A_e}\sqrt{A_c}$	$\sqrt{A_t}$	q_{cr}	Total Heat to Coolant q_t	Corrected Specific Impulse I_{sp} lb-sec/lb	Remarks
																	B/sec in^2	B/sec in^2	B/sec in^2	B/sec in^2	B/sec		
*172	5-30-52	1000-WC-1	WC-1	211-12	2.91	2	989.5	——	1.458	.427	1.885	3.42	——	.3278	5980	——	——	——	——	——	——	——	Minor explosion on shutdown
**173	5-6-52	1000-WC	WC-1	211-1771	5.68	2	999.7	471	1.680	.314	1.990	5.40	237.0	.3280	5000	1.526	——	——	——	——	——	——	Nozzle burned at throat
*174	5-18-52	"	WC-1	"	12.88	5-10	725.0	358	1.265	.244	1.509	5.18	238.0	.3320	5180	1.487	——	——	——	——	——	——	Small crack in chamber by flange weld
*175	5-18-52	"	"	"	36.45	35	706.5	362	1.178	.250	1.428	4.05	233.0	.3260	5060	1.480	4.86	2.65	——	——	——	——	Explosion on shutdown, separated chamber
*176	6-2-52	1000-B-1	B-1	"	10.16	——	——	——	——	——	——	——	——	——	——	——	——	——	——	——	——	——	Nozzle throat severely eroded
*177	6-3-52	1000-B-1	B-1	"	9.14	——	——	——	——	——	——	——	——	——	——	——	——	——	——	——	——	——	" " " "
*178	6-3-52	1000-B-2	B-2	"	2.61	——	——	——	——	——	——	——	——	——	——	——	——	——	——	——	——	——	Flame extinguished when acid flow # epped off
*179	6-5-52	"	"	"	7.87	——	——	——	——	——	——	——	——	——	——	——	——	——	——	——	——	——	Nozzle throat severely eroded
*180	6-5-52	1000-WC2	WC-Cu-1	"	3.00	——	——	——	——	——	——	——	——	——	——	——	——	——	——	——	——	——	Nozzle water flow dropped off
181	6-10-52	"	"	"	24.43	5	1014	493	1.826	.252	2.118	6.253	232.6	.3107	4785	1.565	——	——	——	——	——	——	Nozzle burned
						10-20	1000	468	1.610	.375	1.988	4.293	263.6	.3107	5086	1.558	——	——	——	——	——	——	Oscillation stopped after 6 sec., dark acid
**182	6-17-52	"	WC-Cu-2	"	16.62	10	1006	475	1.853	.285	2.138	6.502	232.2	.3207	4953	1.472	——	3.28	——	——	——	——	Unstable run, nozzle water flow dropped off
183	6-18-52	"	"	"	10.71	10	999.5	470	1.733	.279	2.012	6.211	233.6	.3177	5076	1.480	5.65	——	——	——	——	——	Blew acid injector pressure line
**184	6-18-52	"	"	"	10.89	10	999.5	475	1.795	.300	2.095	5.990	232.1	.3137	4907	1.515	5.03	2.36	3.27	13.6	296.8	257.4	" " " " " " " , unstable run
185	6-23-52	"	"	"	7.84	5	1010	485	1.675	.305	1.980	5.492	245.0	.3137	5146	1.532	——	——	——	——	——	——	Nozzle burned out divergent section
186	7-1-52	"	"	"	4.86	——	——	——	——	——	——	——	——	——	——	——	——	——	——	——	——	——	Flame extinguished
187	7-1-52	"	"	"	39.46	5-15	997.5	498	1.653	.531	2.184	3.113	228.0	.3260	4758	1.531	5.44	2.33	3.40	18.7	290.4	258.3	Good run
						20-30	1014	507	1.671	.516	2.187	3.238	231.8	.3260	4851	1.535	5.34	2.22	3.25	18.1	288.7	257.8	
						35-40	1024	513.5	1.682	.4985	2.180	3.374	235.9	.3260	4927	1.538	5.53	2.16	3.32	18.7	295.0	261.5	
**188	9-19-52	"	WC-Cu-3	"	14.79	5-10	1028	508	1.968	.3326	2.301	5.917	220.8	.3243	4699	1.524	7.52	3.30	4.78	16.4	339.8	229.2	Very rough, unstable
**						13	1002	497	1.782	.3657	2.148	4.873	231.4	.3243	4870	1.528	7.57	3.37	4.84	21.6	349.3	230.2	Unstable
189		"	"	211-672	41.97	5-40	1025	516.2	1.676	.4130	2.089	4.058	246.8	.3273	5166	1.539	7.77	4.20	5.86	42.8	422.7	257.0	Good run
**190	11-8-52	"	"	"	11.39	6	987.5	496.4	1.813	.3391	2.152	5.346	230.6	.3240	4980	1.533	——	2.89	——	18.1	——	——	Unstable, nozzle water flow off scale
191	11-18-52	"	"	"	31.95	5-25	1018	527.8	1.721	.3410	2.062	5.047	255.9	.3247	5257	1.556	8.00	3.77	5.25	28.8	388.1	269.0	Smooth run
						30	1019	526.0	1.766	.3277	2.094	5.389	251.2	.3247	5083	1.550	7.05	2.82	4.30	18.7	328.1	258.6	
192	11-20-52	"	"	"	32.00	——	——	——	——	——	——	——	——	——	——	——	——	——	——	——	——	——	No flow rates
193	11-20-52	"	"	"	30.23	5-25	970.9	482.0	1.549	.4817	2.032	3.216	237.3	.3262	5013	1.527	6.65	3.09	4.60	30.8	362.2	246.6	Good run, acid tank pressure set too low
*194	11-21-52	1000B-3	B-3	211-672	7.60	——	——	——	——	——	——	——	——	——	——	——	——	——	——	——	——	——	Start test, no data
*195	12-12-52	1000WC	WC-Cu-3	"	0	——	——	——	——	——	——	——	——	——	——	——	——	——	——	——	——	——	Explosion on start
*196	2-6-53	1000-B-2	B-2	211-672	7.42	——	——	——	——	——	——	——	——	——	——	——	——	——	——	——	——	——	Start test, no data
197	2-7-53	1000-WC	WC-Cu-3	"	20.71	5-15	1008	505.5	1.694	.3638	2.058	4.656	245.5	.3281	5105	1.547	7.93	4.09	5.44	---	367.8	[illegible].7	Good run, no D-ring coolant
198	2-18-53	"	"	"	40.05	5	998.6	506.7	1.663	.4077	2.070	4.079	244.7	.3252	5045	1.558	6.98	3.26	4.56	22.2	332.1	[illegible].9	Good run
						10-35	993.7	495.8	1.622	.4307	2.053	3.766	241.5	.3252	5062	1.531	6.29	3.14	4.34	21.3	308.5	249.3	
199	2-19-53	"	"	"		5	1001	505.7	1.673	.3698	2.043	4.525	247.5	.3262	5167	1.548	——	3.49	——	26.9	——	——	Good run, nozzle coolant flow rate off scale
						10-20	1002	505.1	1.677	.3760	2.055	4.837	245.8	.3262	5119	1.544	——	3.46	——	26.2	——	——	
*200	2-27-53	"	"	"	29.35	7	999.7	496.5	1.851	.2797	2.131	6.629	233.0	.3229	4856	1.543	5.88	——	——	18.0	——	——	$\sqrt{A_c}$ from oscillograph, stable portion of run
						15	1009	500.7	1.848	.2922	2.140	6.322	236.0	.3229	4882	1.541	5.83	——	——	17.1	——	——	Impure acid, stable portion of run
**						10, 20-25	1015	489.6	1.847	.2538	2.101	7.838	228.6	.3229	4842	1.520	5.97	——	——	18.6	——	——	Unstable portion of run
201	2-27-53	"	"	"	41.65	5	1000	487.3	1.714	.3057	2.020	5.608	241.1	.3229	5183	1.508	6.96	3.09	4.35	16.0	317.1	249.2	Slightly rough
						10	994.2	482.0	1.592	.3560	1.948	4.474	246.9	.3229	5283	1.503	7.51	3.14	4.67	20.8	337.3	255.7	Good run
						15-35	994.4	482.8	1.594	.3669	1.962	4.386	245.6	.3229	5259	1.502	7.04	3.19	4.58	20.3	327.5	252.1	$\sqrt{A_c}$ from oscillograph
**202	2-28-53	"	"	"	39.70	5-10	973.0	470.9	1.880	.2560	2.136	7.344	220.4	.3187	4668	1.518	6.86	2.82	3.98	13.9	283.5	228.0	Unstable period
						15-20	991.1	482.8	1.856	.2719	2.130	6.833	226.6	.3187	4769	1.528	7.32	2.83	4.14	15.3	295.7	236.3	Stable period
**						25-30	975.7	471.1	1.901	.2473	2.148	7.687	219.3	.3187	4696	1.515	6.95	2.88	3.71	14.3	285.3	226.4	Unstable period
203	3-3-53	"	"	"	10.89	5	981.0	466.2	1.531	.5476	2.078	2.795	225.3	.3169	4811	1.506	——	——	——	16.6	——	——	Rough run
						10	982.5	469.0	1.541	.5592	2.100	2.795	225.4	.3169	4768	1.506	6.62	——	——	16.6	——	——	$\sqrt{A_c}$ from oscillograph
204	3-3-53	"	"	"	44.92	5	978.9	486.4	1.648	.3336	1.982	4.980	245.4	.3176	5145	1.538	6.36	3.00	5.14	21.8	369.6	258.9	Good run
						10-45	1010	491.6	1.643	.3371	1.980	4.875	246.2	.3176	5203	1.536	7.68	3.27	4.88	23.2	349.5	257.1	Good run

WC = watercooled
UC = uncooled
G = Viaflex ceramic
B = Boralite ceramic
* = starting up test or mechanical failure
** = unstable run